RSC Advances

PAPER

View Article Online
View Journal | View Issue

Cite this: *RSC Adv.*, 2025, **15**, 23124

Turn-off fluorescence sensing of raloxifene using erythrosine B with detailed spectroscopic and quantum mechanical studies for pharmaceutical and environmental applications†

Samar F. Miski,[a] Ahmed Serag,*[b] Arwa Sultan Alqahtani,[c] Maram H. Abduljabbar,[d] Reem M. Alnemari,[e] Rami M. Alzhrani[e] and Atiah H. Almalki*[fg]

A novel spectrofluorimetric method was developed for the detection of raloxifene based on its ability to quench the native fluorescence of the erythrosine B dye. Upon excitation at 528 nm, erythrosine B exhibits an emission peak at 554 nm, which undergoes concentration-dependent quenching upon interaction with raloxifene. Spectroscopic and thermodynamic studies revealed a static quenching mechanism with a Stern–Volmer constant of 4.87×10^5 M^{-1} and a favorable Gibbs free energy change (ΔG) of -32.45 kJ mol^{-1}. The calculated bimolecular quenching rate constant exceeded the diffusion-controlled limit, further confirming a ground-state complex formation. Job's method confirmed a 1 : 1 stoichiometric ratio, while quantum mechanical calculations elucidated the binding interactions with a binding energy of -0.143391 hartree and a reduction in dipole moment from 14.06 and 21.85 debye for erythrosine B and raloxifene, respectively, to 9.83 debye for the complex. Parameters affecting fluorescence quenching, such as pH, buffer volume, and erythrosine B concentration, were optimized, revealing maximum quenching at pH 4.0 using an acetate buffer, which is explained by the optimal ionization states of both molecules at this pH. The method validation as per ICH guidelines demonstrated linearity (0.1–3.0 μg mL^{-1}, $r^2 = 0.9997$), sensitivity (LOD = 0.0312 μg mL^{-1}), accuracy (100.76% ± 1.277%), and precision (RSD < 1.671%). Analysis of pharmaceutical formulations showed 99.802% ± 0.528% recovery, with no significant difference from the reference HPLC method. The method was successfully applied to spiked plasma and environmental water samples with recoveries of 95.55–103.03% and 94.62–103.30%, respectively. AGREE calculator assessment (0.73) and BAGI (75.0) confirmed the greenness and practical applicability of the method, offering advantages of rapid analysis time (3 min) and minimal organic solvent consumption compared to existing techniques. This erythrosine B-based approach presents a viable alternative for raloxifene determination in resource-limited settings across diverse sample matrices.

Received 20th May 2025
Accepted 23rd June 2025

DOI: 10.1039/d5ra03551a

rsc.li/rsc-advances

1. Introduction

Raloxifene is a second-generation selective estrogen receptor modulator (SERM) that demonstrates tissue-specific activities.[1] Raloxifene exhibits estrogen agonist effects on bone mineral density and lipid metabolism while exerting antagonistic effects on the breast and uterine tissues.[2] It is primarily prescribed for the prevention and treatment of postmenopausal osteoporosis, significantly reducing the risk of vertebral fractures by 30–40%.[3] In women without pre-existing fractures, raloxifene reduces the relative risk of new vertebral fractures by 50%, and in women with pre-existing fractures, the risk reduction is 30% using the 60 mg dose.[3] Additionally, raloxifene has demonstrated a remarkable 76% reduction in the risk of estrogen receptor-positive invasive breast cancer, with a relative risk of 0.24 (95% CI 0.13–0.44; $P < 0.001$).[4] The beneficial effects of the drug

[a]*Pharmacology and Toxicology Department, College of Pharmacy, Taibah University, Medina, Saudi Arabia*
[b]*Pharmaceutical Analytical Chemistry Department, Faculty of Pharmacy, Al-Azhar University, Nasr City 11751, Cairo, Egypt. E-mail: Ahmedserag777@hotmail.com*
[c]*Department of Chemistry, College of Science, Imam Mohammad Ibn Saud Islamic University (IMSIU), P. O. Box 90950, Riyadh 11623, Saudi Arabia*
[d]*Department of Pharmacology and Toxicology, College of Pharmacy, Taif University, P. O. Box 11099, Taif 21944, Saudi Arabia*
[e]*Department of Pharmaceutics and Industrial Pharmacy, College of Pharmacy, Taif University, P. O. Box 11099, Taif 21944, Saudi Arabia*
[f]*Addiction and Neuroscience Research Unit, Health Science Campus, Taif University, P. O. Box 11099, Taif 21944, Saudi Arabia. E-mail: ahalmalki@tu.edu.sa*
[g]*Department of Pharmaceutical Chemistry, College of Pharmacy, Taif University, P. O. Box 11099, Taif 21944, Saudi Arabia*

† Electronic supplementary information (ESI) available. See DOI: https://doi.org/10.1039/d5ra03551a

extend to the cardiovascular system through reduced total and LDL cholesterol levels (12% and 14% reductions, respectively) and lower fibrinogen concentrations (12–14%) without altering HDL cholesterol or triglyceride content.[5] However, raloxifene administration may be associated with adverse effects, including a 44% higher rate of thromboembolic events, leg cramps in 2–4% of patients, and hot flushes in 4–6% of cases, typically during the first 6 months of treatment.[6] From a pharmacokinetic perspective, raloxifene undergoes extensive first-pass metabolism, with only 2% of the administered dose reaching systemic circulation, while approximately 60% is absorbed.[7] The drug is primarily metabolized in the liver to glucuronide conjugates (raloxifene-6-β-glucuronide, raloxifene-4′-β-glucuronide, and raloxifene-6,4′-diglucuronide), which can be reconverted to the active form, thereby extending its biological half-life to 28 hours.[7]

The detection of raloxifene in various matrices is essential for the quality control of pharmaceutical formulations, therapeutic drug monitoring, pharmacokinetic studies, doping control in sports, and environmental assessment. Several analytical methods have been reported for the quantification of raloxifene; however, most of them present significant limitations. High-performance liquid chromatography (HPLC) methods with UV detection have been developed for raloxifene analysis in pharmaceutical formulations;[8–10] however, these approaches typically require lengthy run times, extensive sample preparation, and consume large volumes of organic solvents. Liquid chromatography coupled with tandem mass spectrometry (LC-MS/MS) offers excellent sensitivity for raloxifene detection in biological matrices;[11,12] however, it necessitates sophisticated instrumentation and complex extraction procedures that may not be readily available in many laboratories. Electrochemical methods employing modified electrodes have also been reported,[13] although these techniques often require complex electrode fabrication processes and specialized expertise, limiting their routine application. Interestingly, various spectrofluorimetric approaches have been explored for the detection of raloxifene. For instance, micelle-enhanced methods using sodium dodecyl sulfate (SDS) have been developed to enhance the weak native fluorescence of raloxifene;[14] however, these methods require careful optimization of surfactant concentrations and may suffer from micelle instability. Metal complexation techniques utilizing Al^{3+} have also been employed;[14] however, they require precise pH control and complex formation conditions, as well as consideration of the potential toxicity of Al^{3+}. Recently, nanoparticle-based sensors incorporating gold nanoparticles[15] or metal–organic frameworks[16] have emerged, but their synthesis and optimization can be complex and time-consuming. Furthermore, many of these methods utilize substantial amounts of organic solvents, raising environmental concerns, and lack validation in complex biological matrices or environmental samples.

Fluorescent dyes have emerged as promising probes for pharmaceutical analysis due to their high sensitivity, selectivity, and operational simplicity.[17,18] Among these, xanthene dyes, such as erythrosine B, have garnered attention owing to their superior photophysical properties, including high molar absorptivity and quantum yield.[19,20] These dyes can interact with various analytes through different mechanisms, including static or dynamic quenching, providing a basis for sensitive detection.[21,22] Notably, erythrosine B has demonstrated remarkable sensing capabilities for several compounds through fluorescence quenching mechanisms.[23,24] The interaction between erythrosine B and target analytes can be modulated by optimizing experimental conditions, such as pH, buffer composition, and temperature, enabling highly sensitive and selective detection. When compared to nanoparticle-based sensors, erythrosine B offers advantages of commercial availability, eliminating complex synthesis procedures, consistent batch-to-batch reproducibility, and minimal environmental impact due to reduced reagent consumption. Despite these promising features, the potential of erythrosine B as a fluorescent probe for raloxifene determination remains unexplored.

This study aims to develop a novel turn-off fluorescence sensor based on erythrosine B for the sensitive and selective detection of raloxifene in pharmaceutical formulations, biological samples, and environmental matrices. The research aims to thoroughly investigate the spectral characteristics and quenching mechanism of raloxifene–erythrosine B interactions through spectroscopic techniques, Stern–Volmer analysis, thermodynamic studies, and Job's method. Quantum mechanical calculations will be used to elucidate binding sites, energies, and interaction parameters. Experimental conditions, including the pH, buffer composition, erythrosine B concentration, and reaction time, will be optimized to enhance analytical performance. The method will be validated according to the ICH guidelines, assessing linearity, sensitivity, accuracy, precision, robustness, and selectivity. The practical applicability will be demonstrated through the analysis of pharmaceutical formulations, spiked plasma samples, and environmental water matrices. The environmental impact and analytical efficiency will be evaluated using greenness and blueness assessment tools. This approach is expected to overcome the limitations of the existing analytical methods by offering simplicity, rapidity, superior sensitivity, and enhanced environmental sustainability while maintaining robust performance across diverse sample matrices. The proposed erythrosine B-based fluorescence sensor offers significant advantages over conventional techniques, including minimal reagent consumption, reduced instrumentation costs, and shortened analysis times, posing a viable alternative for raloxifene detection in resource-limited settings.

2. Experimental

2.1. Materials and reagents

Raloxifene standard (99.9% purity) was obtained from the Egyptian Drug Authority (Cairo, Egypt). Pharmaceutical formulations containing raloxifene (Evista® tablets, 60 mg raloxifene) were purchased from local pharmacies (Cairo, Egypt). Erythrosine B dye (95% dye content) and HPLC grade ethanol were procured from Sigma-Aldrich (St. Louis, MO, USA). Buffer reagents, including sodium hydroxide, hydrochloric acid, potassium chloride, phosphoric acid, mono and di-

sodium phosphate salts, sodium acetate, and acetic acid, were of analytical grade and purchased from El-Nasr Chemical Company (Cairo, Egypt). Distilled water was utilized for the preparation of all solutions. Human plasma samples were purchased from VACSERA CO., Giza, Egypt, and stored at −20 °C until analysis.

Erythrosine B was prepared as a 0.02% w/v stock solution in distilled water. Buffer solutions, including hydrochloric acid–potassium chloride buffer (pH 3–3.5), acetate buffer (pH 4–5.5), and phosphate buffer (pH 6.0–7.0), were prepared according to the USP guidelines.

2.2. Instrumentation

A Shimadzu UV-1800 double-beam UV-vis spectrophotometer with matched 1 cm quartz cells was used for spectrophotometric measurements. Fluorescence measurements were performed using a Jasco FP-6200 spectrofluorometer equipped with a 150 W xenon lamp and 1.0 cm quartz cells. The parameters were optimized as follows: excitation wavelength was set at 527 nm, and the emission spectra were recorded between 540 and 650 nm. The slit widths for both excitation and emission were set at 10 nm, and the scan speed was maintained at 3000 nm min^{-1}. pH measurements were conducted using a calibrated Jenway 3510 pH meter (Staffordshire, UK). Computational calculations were performed using the Gaussian 09 software package (Gaussian Inc., Wallingford, CT, USA).

2.3. Standard solutions and construction of the fluorescent probe

A stock solution of raloxifene (100 μg mL^{-1}) was prepared by dissolving 10 mg of raloxifene in 10 mL of ethanol, and the solution was made up to 100 mL with distilled water to obtain a final concentration of 100 μg mL^{-1}. The working standard solution (20 μg mL^{-1}) was prepared by diluting 10 mL of the stock solution with a mixture of ethanol and distilled water (1 : 10 v/v) to a final volume of 50 mL, maintaining the same solvent ratio as the stock solution.

For the construction of the fluorescent probe, 1 mL of erythrosine B solution (0.02% w/v) was mixed with 1.5 mL of acetate buffer (pH 4.0) in a 10 mL volumetric flask and diluted with distilled water. The excitation and emission wavelengths were set at 528 nm and 554 nm, respectively. The fluorescence intensity of this solution (F_0) was measured before the addition of the analyte.

For the calibration standards, aliquots of the raloxifene working standard solution (20 μg mL^{-1}) corresponding to the final concentrations of 0.1–3.0 μg mL^{-1} were transferred into a series of 10 mL volumetric flasks. One mL of erythrosine B (0.02% w/v, final concentration 20.0 μg mL^{-1}) was added to each flask, followed by 1.5 mL of acetate buffer (pH 4.0). The solutions were then diluted to the mark with distilled water and mixed well. After 3 minutes of incubation at room temperature, the fluorescence intensity (F) of each solution was measured. The quenching ratio, expressed as F_0/F, was plotted against the corresponding raloxifene concentration to construct the calibration curve.

2.4. Quantum mechanical calculations

The quantum mechanical calculations were conducted using the Gaussian 09 software package. Initial geometries of raloxifene, erythrosine B, and their potential complex were built using the GaussView 6.0 molecular visualization program. The geometries were then optimized using the semi-empirical PM3 method due to its computational efficiency and reasonable accuracy for large molecular systems.

The binding energy between raloxifene and erythrosine B was estimated using the following equation:

$$\Delta E = E(\text{complex}) - E(\text{raloxifene}) - E(\text{erythrosine B})$$

E(complex), E(raloxifene), and E(erythrosine B) represent the total energies of the optimized structures for the complex, raloxifene, and erythrosine B, respectively. Additionally, dipole moments and polarizability were calculated to further elucidate the nature of the interaction.

2.5. Method validation

The developed spectrofluorimetric method was validated according to the International Conference on Harmonization (ICH) guidelines Q2(R2).[25] The validation parameters included linearity, limits of detection and quantification, accuracy, precision, selectivity, and robustness. Detailed validation procedures are provided in the ESI.†

2.6. Application to pharmaceutical formulations, spiked plasma, and environmental samples

2.6.1. Analysis of pharmaceutical formulations. The developed erythrosine B fluorescence quenching method was applied to determine raloxifene in commercial tablet formulations. Ten tablets were accurately weighed, finely powdered, and an amount equivalent to 10 mg of raloxifene was transferred to a 100 mL volumetric flask. The powder was dissolved in 10 mL of ethanol using sonication for 15 minutes to ensure complete dissolution. The solution was then diluted to the mark with distilled water, filtered through a 0.45 μm membrane filter, and further diluted to obtain the required working concentration. The analysis was performed as per the optimized procedure, and the raloxifene content was determined by referring to the previously constructed calibration curve. The results were statistically compared with those obtained by a reported HPLC method using Student's t-test, F-test and interval hypothesis testing at a 95% confidence level.

2.6.2. Analysis of spiked human plasma samples. For the analysis of raloxifene in biological matrices, 1 mL of drug-free human plasma samples was spiked with different concentrations of the raloxifene standard solution to obtain initial concentrations of 2.0, 5.0, 10.0, and 20.0 μg mL^{-1}. Protein precipitation was performed using acetonitrile (1 : 2 ratio), followed by centrifugation at 5000 rpm for 15 minutes at 4 °C. The supernatants were evaporated under nitrogen, reconstituted with a 2 mL ethanol : water (50 : 50 v/v) solution, vortexed for 30 seconds to ensure complete dissolution, and filtered through 0.22 μm syringe filters to remove any particulate matter.

For fluorescence analysis, 1 mL of each filtered solution was transferred to a 10 mL volumetric flask according to the general procedure previously mentioned. Considering all dilution steps, the final concentrations in the measured solutions were 0.2, 0.5, 1.0, and 2.0 μg mL^{-1}, corresponding to the initial plasma concentrations of 2.0, 5.0, 10.0, and 20.0 μg mL^{-1}, respectively.

A calibration curve specifically for plasma analysis was constructed by processing drug-free plasma spiked with known concentrations of raloxifene (0.1–3.0 μg mL^{-1}) through the same extraction procedure. Blank plasma samples were processed similarly and used for background correction to account for any matrix effects.

2.6.3. Analysis of environmental water samples. For the analysis of raloxifene in environmental matrices, water samples (river water and tap water) were initially filtered through 0.45 μm membrane filters to remove particulate matter. One mL of each filtered water sample was spiked with the raloxifene standard solution to achieve initial concentrations of 2.0, 5.0, 10.0, and 20.0 μg mL^{-1}. A salting-out liquid–liquid extraction procedure was employed for sample clean-up and preconcentration. To each spiked water sample, 2 mL of ethanol was added, followed by the addition of 300 mg of sodium chloride to induce phase separation. The mixtures were vortexed vigorously for 1 minute and then centrifuged at 5000 rpm for 10 minutes.

The upper ethanol-rich layer was carefully collected and filtered through 0.22 μm syringe filters. For fluorescence analysis, 1 mL of each filtered solution was transferred to a 10 mL volumetric flask according to the general procedure previously mentioned. Considering all dilution steps, the final concentrations in the measured solutions were 0.2, 0.5, 1.0, and 2.0 μg mL^{-1}, corresponding to the initial water concentrations of 2.0, 5.0, 10.0, and 20.0 μg mL^{-1}, respectively.

A calibration curve specifically for environmental analysis was constructed by processing water samples spiked with known concentrations of raloxifene (0.1–3.0 μg mL^{-1}) through the same extraction procedure. Blank water samples were processed similarly and used for background correction to account for any matrix effects.

3. Results and discussion

3.1. Spectral characteristics

The interaction between erythrosine B and raloxifene was thoroughly investigated through spectroscopic studies to establish the fundamental basis for the proposed analytical method (Fig. 1). Erythrosine B is a xanthene dye characterized by a conjugated π-electron system containing four iodine atoms that enhance its chromophoric and fluorophoric properties. This structural configuration contributes to its spectroscopic properties, including high molar absorptivity and quantum yield.

The absorption spectrum of erythrosine B (Fig. 1A) exhibited a characteristic peak at 527 nm, attributed to the $\pi \rightarrow \pi^*$ transitions within the xanthene ring system. This intense absorption band in the visible region is responsible for the distinctive red color of the dye in solution. Interestingly, when raloxifene was added to the erythrosine B solution, significant spectral changes were observed in the absorption profile (Fig. 1A). The primary peak at 527 nm showed a pronounced hypochromic effect (decreased intensity), while a new shoulder peak emerged at approximately 490 nm. This spectral alteration suggests the formation of a new molecular complex with distinct electronic properties. The appearance of the shoulder peak could be attributed to the perturbation of the π-electron system of erythrosine B upon complexation with raloxifene. These spectral changes provide strong evidence for the formation of a ground-state complex rather than collisional interactions.

The fluorescence behavior of erythrosine B and its interaction with raloxifene were also examined using spectrofluorimetric measurements. The excitation and emission spectra of erythrosine B show maximum excitation at 528 nm and emission at 554 nm (Fig. 1B). This Stokes shift (26 nm) provides a sufficient spectral window between excitation and emission, minimizing self-absorption effects and making erythrosine B an appropriate candidate for fluorescence-based analytical applications. The emission at longer wavelengths is particularly advantageous for analyzing complex biological and environmental samples, as it reduces potential interference from endogenous fluorophores that typically emit at shorter wavelengths. Upon the sequential addition of raloxifene, a concentration-dependent quenching of erythrosine B fluorescence was observed (Fig. 1C). The significant reduction in fluorescence intensity without a shift in emission wavelength is consistent with the formation of a non-fluorescent complex that reduces the concentration of free erythrosine B molecules available for excitation. This remarkable quenching effect provides the analytical basis for the quantitative determination of raloxifene.

3.2. Fluorescence quenching mechanism

The fluorescence quenching mechanism between erythrosine B and raloxifene was systematically investigated to understand the nature and strength of their interaction. Stern–Volmer analysis was employed as a primary tool to distinguish between static and dynamic quenching mechanisms.

As shown in Fig. 2A, the Stern–Volmer plot exhibited excellent linearity ($R^2 = 0.9998$) with a K_{SV} value of 4.87×10^5 M^{-1}. The linearity of this plot suggests a predominant single type of quenching mechanism rather than a combination of different processes. To further distinguish between static and dynamic quenching, the bimolecular quenching rate constant (k_q) was calculated using the reported fluorescence lifetime of erythrosine B (89 ps).[26] The calculated k_q value was 5.48×10^{14} M^{-1} s^{-1}, which significantly exceeds the diffusion-controlled limit (2.0×10^{10} M^{-1} s^{-1}) by four orders of magnitude. This finding strongly indicates that the quenching process cannot be attributed to diffusion-controlled collisional encounters between erythrosine B and raloxifene, but rather to the formation of a non-fluorescent ground-state complex. This conclusion is consistent with the spectral changes observed in the absorption spectrum, reinforcing the static quenching mechanism.

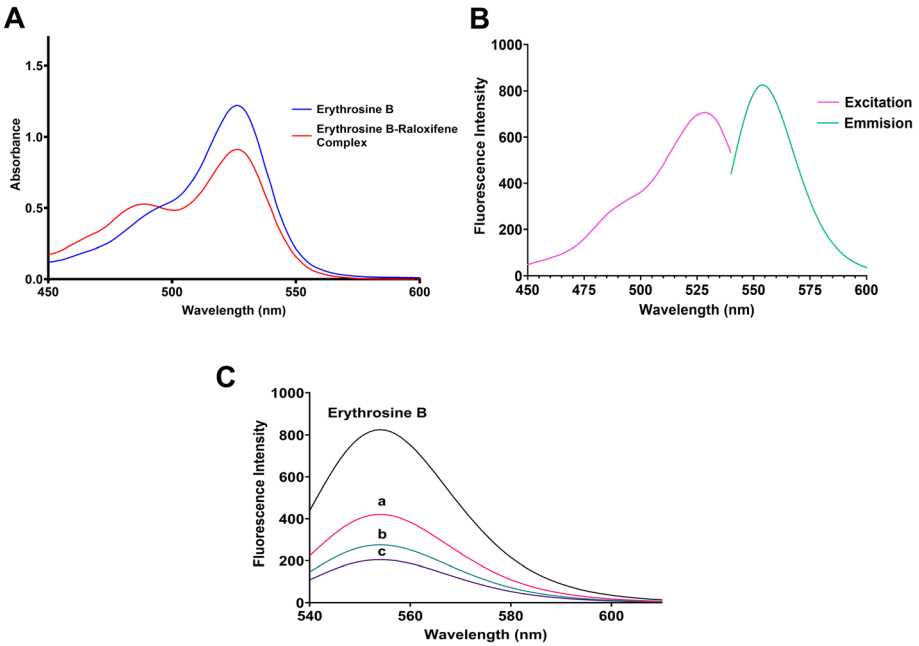

Fig. 1 (A) Absorption spectra of erythrosine B in the absence and presence of raloxifene show a hypochromic effect at 527 nm and the emergence of a new shoulder peak at approximately 490 nm upon complex formation; (B) excitation and emission spectra of erythrosine B show maximum excitation at 528 nm and emission at 554 nm; (C) emission spectra of erythrosine B show concentration-dependent quenching upon the addition of increasing concentrations of raloxifene: (a) 1.0 μg mL^{-1}, (b) 2.0 μg mL^{-1}, and (c) 3.0 μg mL^{-1} at pH 4.0, demonstrating the turn-off fluorescence sensing mechanism.

The association constant (K_a) for the complex formation was determined using the modified Stern–Volmer equation:

$$F_0/(F_0 - F) = 1 + 1/(K_a[Q])$$

The association constant (K_a) was calculated to be 4.10×10^5 M^{-1}, indicating a high affinity between erythrosine B and raloxifene. This strong interaction is beneficial for developing a sensitive analytical method, as it enhances the responsiveness of the method to small changes in raloxifene concentration.

The thermodynamic feasibility of the interaction was assessed by calculating the Gibbs free energy change (ΔG) at 298 K using the equation:

$$\Delta G = -2.303RT \log K_a$$

The ΔG value was found to be -32.45 kJ mol^{-1}, confirming the spontaneity of the complex formation process. The substantial negative value of ΔG suggests that the interaction between erythrosine B and raloxifene is energetically favorable

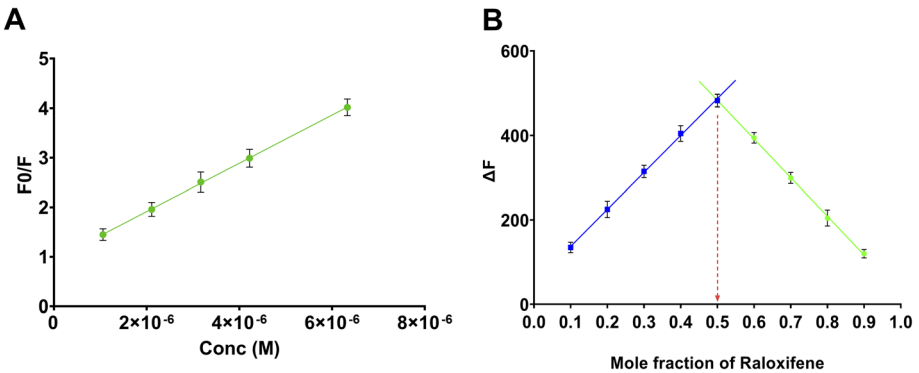

Fig. 2 (A) Stern–Volmer plot for the interaction between erythrosine B and raloxifene at pH 4.0 and room temperature, demonstrating a linear relationship with $K_{SV} = 4.87 \times 10^5$ M^{-1}; (B) Job's plot for the determination of erythrosine B–raloxifene complex stoichiometry, showing maximum fluorescence change at 0.5 mole fraction, confirming 1 : 1 binding ratio. Error bars represent standard deviation from triplicate measurements ($n = 3$).

and thermodynamically stable under the experimental conditions.

To determine the stoichiometry of the erythrosine B–raloxifene complex, Job's method of continuous variation was employed. In this approach, the total molar concentration of erythrosine B and raloxifene was maintained at 6×10^{-6} M, while their mole fractions were systematically varied. The difference in fluorescence intensity (ΔF) was plotted against the mole fraction of raloxifene (Fig. 2B). The maximum fluorescence change occurred at a mole fraction of 0.5, clearly indicating the formation of a 1 : 1 complex between erythrosine B and raloxifene. This finding is particularly important for understanding the binding mechanism and for developing a robust analytical method with predictable stoichiometric relationships.

Collectively, these results provide comprehensive evidence that the fluorescence quenching of erythrosine B by raloxifene primarily occurs through a static quenching mechanism involving the formation of a thermodynamically stable 1 : 1 ground-state complex. The high association constant and favorable free energy change confirm the strong and spontaneous nature of this interaction, providing an excellent foundation for the development of a sensitive and selective analytical method for the detection of raloxifene.

3.3. Quantum mechanical calculations

Semi-empirical PM3 calculations were performed to provide deeper insights into the molecular-level interactions between erythrosine B and raloxifene. The energetic and electronic parameters derived from these calculations are summarized in Table 1, offering quantitative evidence for the nature and strength of the complex formation.

The computational results in Table 1 reveal significant differences in the electronic properties of the individual molecules compared to their complex. The total energy (E(PM3)) of the complex (−0.050016 hartree) is lower than the sum of the individual components (−0.035415 hartree for erythrosine B and 0.128790 hartree for raloxifene), resulting in a binding energy (ΔE) of −0.143391 hartree. This substantially negative ΔE indicates a highly favorable energetic interaction between the two molecules, confirming the intrinsic stability of the complex, independent of solvent effects. The most remarkable electronic alteration upon complex formation is the substantial decrease in dipole moment from the individual molecules (14.06 and 21.85 debye for erythrosine B and raloxifene, respectively) to 9.83 debye for the complex. This dramatic decrease reflects the complementary charge distribution in the complex, where the negative charge of erythrosine B (−1) effectively neutralizes the positive charge of raloxifene (+1) at the optimized pH. Conversely, the polarizability of the complex (566.10 a.u.) shows a remarkable enhancement compared to the individual molecules (301.67 and 270.84 a.u. for erythrosine B and raloxifene, respectively). This increased polarizability suggests extensive electronic delocalization across the entire complex, contributing to its stability and distinct spectroscopic properties.

The molecular structures illustrated in Fig. 3 elucidate the specific binding interactions between the fluorophore and the analyte. The individual molecules, erythrosine B (Fig. 3A) and raloxifene (Fig. 3B), display distinctive structural features that facilitate their interaction. Erythrosine B exhibits a planar xanthene core decorated with four iodine atoms and a pendant carboxylate group, while raloxifene presents a complex three-dimensional architecture featuring a central benzothiophene scaffold with hydroxyl-substituted phenyl rings and a basic piperidine moiety. The optimized complex structure (Fig. 3C) reveals two dominant non-covalent interactions that govern the association between these molecules. The first critical interaction is a hydrogen bond that is formed between the carbonyl oxygen of the erythrosine B carboxylate group and a hydrogen in

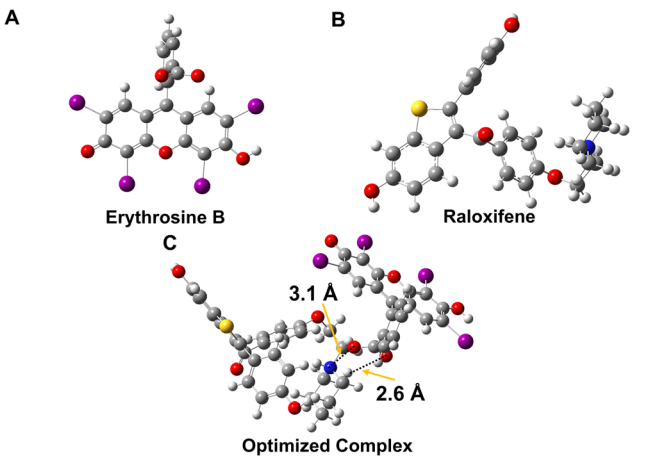

Fig. 3 (A) Optimized structure of erythrosine B shows the xanthene ring system with iodine atoms and carboxylate group; (B) optimized structure of raloxifene highlighting the benzothiophene scaffold, phenolic groups, and piperidine moiety; (C) optimized geometry of the erythrosine B–raloxifene complex shows key binding interactions, including hydrogen bonding (2.6 Å) and electrostatic attraction (3.1 Å).

Table 1 Quantum mechanical parameters derived from PM3 calculations for erythrosine B, raloxifene, and their molecular complex

Parameter	Erythrosine B	Raloxifene	Erythrosine B–raloxifene complex
Charge	−1	1	0
E(RPM3) (hartree)	−0.035415	0.128790	−0.050016
RMS gradient norm (hartree per bohr)	0.000002	0.000001	0.000002
Dipole moment (debye)	14.064400	21.853597	9.827947
Polarizability (α) (a.u.)	301.666667	270.836000	566.095000

raloxifene, with a precisely measured interatomic distance of 2.6 Å. This distance falls within the optimal range for strong hydrogen bonding, contributing significantly to the stability of the complex. The second key interaction, visualized at a distance of 3.1 Å in Fig. 3C, is an electrostatic attraction between the negatively charged oxygen of the erythrosine B carboxylate group and the positively charged nitrogen in the piperidine moiety of raloxifene. This ionic interaction is particularly crucial at the experimentally optimized pH of 4.0, where the piperidine nitrogen of raloxifene exists predominantly in its protonated form while the carboxylate group of erythrosine B remains substantially deprotonated, creating ideal conditions for charge-based attraction. Additionally, the optimized geometry demonstrates a favorable spatial arrangement where the planar xanthene core of erythrosine B aligns with the benzothiophene scaffold of raloxifene, establishing extensive π–π stacking interactions that provide additional stabilization. This structural alignment maximizes the overlap between the π-electron systems of both molecules, confirming the polarizability results that indicate extensive electronic delocalization.

These quantum mechanical insights provide a structural foundation for understanding the fluorescence quenching mechanism. The identified interactions create an efficient non-radiative energy dissipation pathway, which explains the effective quenching observed experimentally and validates the proposed static quenching mechanism that underpins the analytical method developed in this study.

3.4. Method optimization

The analytical performance of the proposed method was systematically optimized by investigating various parameters that potentially influence the fluorescence quenching of erythrosine B by raloxifene.

3.4.1. Effect of pH and buffer type. The pH of the reaction medium plays a critical role in the fluorescence quenching efficiency of erythrosine B by raloxifene, as it directly influences the ionization state of both interacting molecules. As shown in Fig. 4A, the quenching efficiency (F_0/F) was investigated over a pH range of 3.0–7.0 using appropriate buffer systems, including hydrochloric acid–potassium chloride buffer (pH 3–3.5), acetate buffer (pH 4–5.5), and phosphate buffer (pH 6.0–7.0). The results revealed a significant pH dependence, with the maximum quenching efficiency observed at pH 4.0, followed by a plateau between pH 4.5–6.0, and then a slight decrease at pH 7.0.

This pH-dependent behavior can be explained by examining the computational pK_a values of both molecules (Fig. S1 and S2†), as calculated using Marvin Sketch software (version 24.3.2, Chemaxon) (**https://www.chemaxon.com**). Erythrosine B contains a carboxylic acid group with a pK_a of 3.52, which becomes increasingly deprotonated as the pH rises above 3.0, reaching significant ionization at pH 4.0. Concurrently, the piperidine nitrogen in raloxifene (pK_a 8.38) remains predominantly protonated across the studied pH range, while the phenolic groups (pK_a 9.58 and 8.99) remain largely unionized. At pH 4.0, the optimal electrostatic interaction occurs between the negatively charged carboxylate of erythrosine B and the positively charged piperidine nitrogen of raloxifene, facilitating the strongest complex formation. At lower pH values (<4.0), insufficient ionization of the erythrosine B carboxylate reduces the electrostatic attraction. Conversely, at higher pH values (>6.0), partial deprotonation of phenolic groups in raloxifene begins to diminish its net positive charge, weakening the interaction. Therefore, acetate buffer at pH 4.0 was selected for subsequent experiments.

3.4.2. Effect of buffer volume. The volume of acetate buffer (pH 4.0) added to the reaction mixture was examined in the range of 0.5–3.5 mL in a final volume of 10 mL (Fig. 4B). The quenching efficiency increased progressively with increasing buffer volume up to 1.5 mL, after which it plateaued between 1.5–2.5 mL, followed by a slight decrease at 3.5 mL. The observed pattern can be explained by considering the buffer capacity. At low buffer volumes (<1.0 mL), insufficient buffering capacity fails to maintain the optimal pH environment throughout the reaction medium, resulting in suboptimal complex formation. The plateau region (1.5–2.5 mL) represents the optimal buffer capacity, where pH stability is maintained without interference from the interactions. The slight decrease in quenching efficiency at higher buffer volumes (>3.0 mL) might be attributed to the increased ionic strength, which could potentially compete with the electrostatic interactions between raloxifene and erythrosine B or alter the solvation shell around the interacting molecules. Based on these findings, 1.5 mL of acetate buffer was selected as the optimal volume, providing maximum quenching efficiency with minimal reagent consumption.

3.4.3. Effect of erythrosine B concentration. The concentration of erythrosine B was investigated in the range of 10.0–60.0 μg mL^{-1} (corresponding to 0.5–3.0 mL of 0.02% w/v solution) (Fig. 4C). The quenching efficiency increased sharply with increasing erythrosine B concentration up to 20.0 μg mL^{-1}, followed by a plateau between 20.0–40.0 μg mL^{-1}, and a slight decrease at 60.0 μg mL^{-1}. This trend reflects the complex interplay between the fluorophore concentration and the quenching dynamics. At low erythrosine B concentrations (<20.0 μg mL^{-1}), the limited availability of fluorophore molecules results in reduced sensitivity for raloxifene detection. The plateau region (20.0–40.0 μg mL^{-1}) represents the optimal concentration range where sufficient fluorophore molecules are available for interaction with raloxifene without excess reagent, ensuring efficient and accurate detection. The slight decrease in quenching efficiency at higher concentrations (>40.0 μg mL^{-1}) can be attributed to potential self-quenching effects of erythrosine B molecules at elevated concentrations, where intermolecular interactions between the excess dye molecules may compete with the raloxifene–erythrosine B interaction. Consequently, 20.0 μg per mL erythrosine B concentration (1.0 mL of 0.02% w/v solution) was selected as optimal for subsequent analyses, offering maximum sensitivity while minimizing potential interferential effects.

3.4.4. Effect of reaction time. The kinetics of the interaction between erythrosine B and raloxifene was investigated by

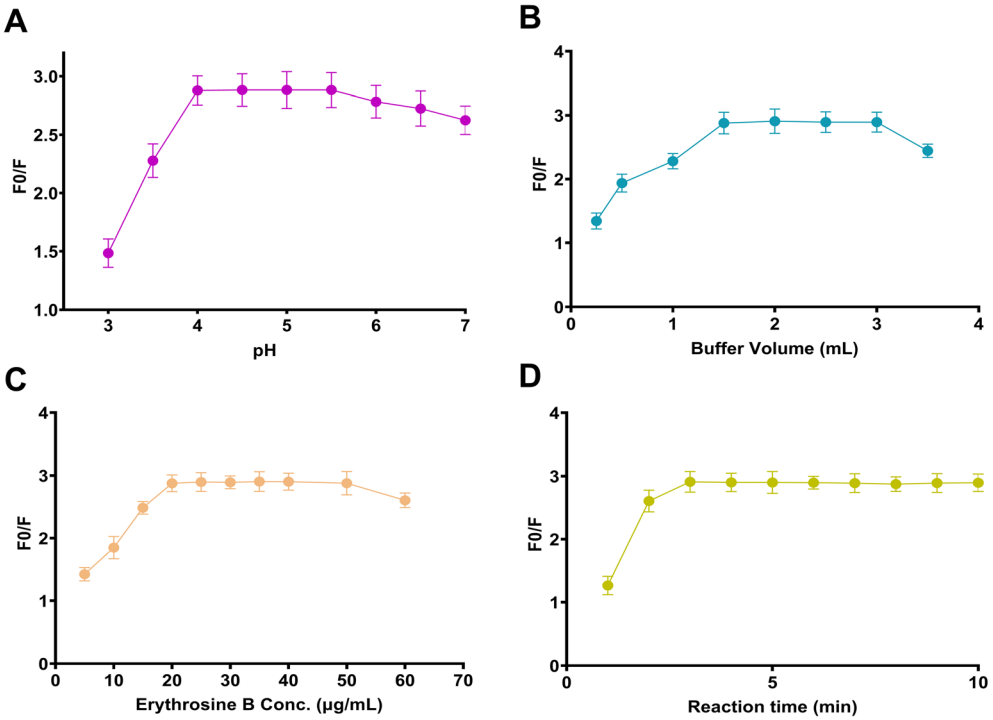

Fig. 4 (A) Effect of pH on quenching efficiency, with maximum quenching at pH 4.0; (B) effect of buffer volume on quenching efficiency shows optimal performance at 1.5 mL; (C) effect of erythrosine B concentration, with maximum response at 20.0 μg mL^{-1} (corresponding to 1.0 mL of 0.02% w/v solution); (D) time-dependent quenching efficiency demonstrating rapid equilibration within 3 minutes, followed by signal stability. Error bars represent standard deviation from triplicate measurements ($n = 3$).

monitoring fluorescence quenching as a function of time after mixing the reagents (Fig. 4D). The quenching process exhibited rapid kinetics, reaching maximum efficiency within 3 minutes and remaining stable for at least 10 minutes. This rapid equilibration is characteristic of the static quenching mechanism previously established, where ground-state complex formation occurs almost instantaneously upon molecular contact. The stabilization of the signal after 3 minutes confirms the formation of a thermodynamically stable complex that maintains its integrity over an extended period. The rapid reaction kinetics is advantageous for analytical applications, allowing for high sample throughput without compromising measurement reliability. Consequently, a reaction time of 3 minutes was adopted for subsequent experiments, providing a balance between analytical efficiency and ensuring complete equilibration of the system.

3.5. Method validation

The proposed method was validated in accordance with the ICH Q2(R2) guidelines to ensure its reliability for the intended analytical applications in terms of linearity, sensitivity, accuracy, precision, robustness, and selectivity. The method demonstrated linearity in the concentration range of 0.1–3.0 μg mL^{-1}, with a correlation coefficient (r^2) of 0.9997, as shown in Table 2. The calibration curve is described by the equation $F_0/F = 1.0206C + 0.9594$, where C is the raloxifene concentration in μg mL^{-1}. The high correlation coefficient indicates a strong linear relationship between the quenching signal and analyte concentration, confirming the reliability of the method across the entire working range. The sensitivity of the method was evaluated by determining the limit of detection (LOD) and limit of quantification (LOQ) values, which were calculated as 0.0312 μg mL^{-1} and 0.0937 μg mL^{-1}, respectively. These low values

Table 2 Analytical performance parameters for the developed fluorescence quenching method for raloxifene determination

Parameters		Raloxifene
Excitation wavelength (nm)		528
Emission wavelength (nm)		554
Linearity range (μg mL^{-1})		0.1–3.0
Slope		1.0206
Intercept		0.9594
Correlation coefficient (r^2)		0.9997
LOD (μg mL^{-1})		0.0312
LOQ (μg mL^{-1})		0.0937
Accuracy (% R)[a]		100.76 ± 1.277
Repeatability precision (% RSD)[b]		1.267
Intermediate precision (% RSD)[c]		1.671
Robustness (% R)	Buffer (pH)	101.57 ± 1.332
	Buffer volume (mL)	98.88 ± 0.907
	Erythrosine B volume (mL)	101.39 ± 0.873

[a] Average of 9 determinations (3 concentrations repeated 3 times). [b] % RSD of 9 determinations (3 concentrations repeated 3 times) measured on the same day. [c] % RSD of 9 determinations (3 concentrations repeated 3 times) measured over three consecutive days.

reflect the high sensitivity of the erythrosine B fluorescence quenching approach, making the method suitable for trace analysis of raloxifene in various matrices. The sensitivity was favorable compared to several previously reported methods for raloxifene detection, including HPLC methods with UV detection that typically display LOD values in the range of 0.075–0.100 μg mL^{-1}.

The accuracy of the method was thoroughly assessed by recovery studies at three different concentration levels (0.5, 1.5, and 2.5 μg mL^{-1}) with three replicates each, yielding a mean recovery of 100.76% ± 1.277% (Table 2). This recovery rate falls within the generally accepted range of 98–102%, confirming the ability of the method to provide results that closely approximate the true concentration of raloxifene in samples. Precision was evaluated through both repeatability (intra-day precision) and intermediate precision (inter-day precision) studies. The repeatability, determined by analyzing three concentration levels three times each on the same day, yielded an RSD of 1.267%. The intermediate precision evaluated over three consecutive days resulted in an RSD of 1.671%. These RSD values, below the generally accepted limit of 2%, verify the precision and reliability of the method for routine analytical applications.

The method demonstrated satisfactory robustness when subjected to deliberate minor variations in critical parameters, as evidenced by the minimal impact on recovery rates when the buffer pH (101.57% ± 1.332%), buffer volume (98.88% ± 0.907%), and erythrosine B volume (101.39% ± 0.873%) were varied within the defined ranges (Table 2). These results confirm that the method remains reliable despite minor experimental fluctuations that might occur during routine analysis. The selectivity of the method was confirmed through comprehensive interference studies involving common pharmaceutical excipients, inorganic ions, and biological components. As illustrated in Fig. 5, all tested potential interferents showed negligible quenching efficiency percentage (QE%) compared to raloxifene, with values below 3% *versus* 48% for raloxifene at the same concentration. This high selectivity was observed even in complex biological matrices, such as pooled plasma, demonstrating that the specific interaction between erythrosine B and raloxifene remains largely unaffected by matrix components. This selectivity can be attributed to the unique molecular recognition between erythrosine B and raloxifene, which is governed by both electrostatic and hydrogen bonding interactions as elucidated in the quantum mechanical calculations.

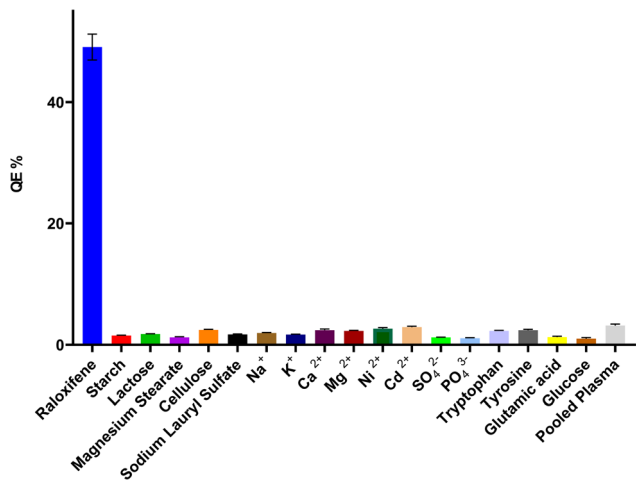

Fig. 5 Selectivity studies show the quenching efficiency percentage (QE%) of various potential interferents compared to raloxifene (1.5 μg mL^{-1}), demonstrating high selectivity with interferent responses below 3% *versus* 48% for raloxifene under identical conditions. Error bars represent standard deviation from triplicate measurements ($n = 3$).

3.6. Method application

The validated fluorescence quenching method was applied to various matrices to demonstrate its practical utility in pharmaceutical, biological, and environmental analyses.

3.6.1. Analysis of pharmaceutical formulations. The proposed method was applied to determine raloxifene in commercial tablets (Evista®). Results showed that the mean content of raloxifene in the analyzed tablets was 99.802% of the labeled amount with a standard deviation of 0.528% (Table 3). For comparison, a reported HPLC method[8] was also employed to analyze the same samples, yielding a mean content of 98.997% with a standard deviation of 0.695%.

A statistical comparison between the two methods was performed using Student's *t*-test and *F*-test at a 95% confidence level. The calculated *t*-value (2.062) was lower than the tabulated value (2.306), indicating no significant difference in accuracy between the two methods. Similarly, the calculated *F*-value (1.736) was lower than the tabulated value (6.338), confirming no significant difference in precision. Additionally, interval hypothesis testing was conducted to further assess the equivalence between the proposed and reference methods. The calculated lower (θ_L) and upper (θ_U) limits were −0.095 and 1.704, respectively. Since both values fell within the acceptable bias limits of ±2%, the results confirm that any differences between the methods are not analytically significant.

3.6.2. Analysis of biological and environmental samples. The applicability of the method to biological matrices was evaluated by analyzing raloxifene in spiked human plasma samples. As shown in Table 4, raloxifene was successfully determined at four concentration levels (0.2, 0.5, 1.0, and 2.0 μg mL^{-1}) with recovery rates ranging from 95.55% to 103.03% and RSD values between 0.951% and 3.428%. The protein precipitation technique using acetonitrile in a 1 : 2 ratio proved effective in removing potential interfering components while maintaining satisfactory analyte recovery. This approach offers several advantages, including simplicity, speed, and reduced consumption of organic solvents.

The method was further applied to determine raloxifene in environmental water samples, including tap water and river water (Table 4). Spiked water samples at four concentration levels (0.2, 0.5, 1.0, and 2.0 μg mL^{-1}) were analyzed after extraction using a salting-out assisted liquid–liquid extraction procedure. Recovery rates ranged from 94.62% to 103.30% for tap water and from 96.53% to 101.60% for river water, with RSD

Table 3 Statistical comparison between the developed fluorescence quenching method and a reported HPLC method for raloxifene determination in pharmaceutical formulations

Method	Mean[a]	SD	t-Test (2.306)[b]	P value	F-Value (6.338)[b]	P value	θ_L[c]	θ_U[c]
Developed method	99.802	0.528	2.062	0.076	1.736	0.607	−0.095	1.704
Reported method	98.997	0.695						

[a] Average of five determinations. [b] The values in parentheses are tabulated values of "t" and "F" at ($P = 0.05$). [c] Bias of ±2% is acceptable.

Table 4 Application of the developed method to spiked biological (plasma) and environmental (river and tap water) samples

Samples	Spiked (μg mL^{-1})	Found (μg mL^{-1})	Recovery (%)	RSD ($n = 3$, %)
Plasma	0.2	0.204	102.13	3.343
	0.5	0.478	95.55	3.428
	1.0	0.985	98.55	0.951
	2.0	2.061	103.03	1.416
River water	0.2	0.194	96.98	3.2416
	0.5	0.483	96.53	3.2881
	1.0	1.016	101.6	1.7097
	2.0	1.942	97.11	0.3757
Tap water	0.2	0.189	94.62	3.2257
	0.5	0.498	99.53	2.8507
	1.0	0.979	97.86	0.9411
	2.0	2.066	103.3	0.4693

values below 3.29% in both matrices, indicating excellent accuracy and precision. The salting-out extraction technique employed offers significant advantages for environmental analysis. The addition of sodium chloride (300 mg) to the water–ethanol mixture creates phase separation through the "salting-out" effect, where water molecules preferentially form hydration shells around salt ions, reducing their availability to solvate organic molecules and forcing them into the ethanol-rich phase. This phenomenon increases the partition coefficient of raloxifene into the organic phase, enhancing extraction efficiency. Additionally, using ethanol as the extracting solvent instead of conventional chlorinated organic solvents, such as dichloromethane or chloroform, significantly reduces environmental and health hazards associated with the extraction process.

3.7. Comparison with previously reported methods

To assess the analytical performance of the developed method, a comprehensive comparison was conducted with previously reported methods for raloxifene determination (Table S1†). The developed erythrosine B fluorescence quenching method offers several advantages compared to previously reported methods. In contrast to HPLC methods, a reduced analysis time (3 min *versus* 5.32–10.6 min for HPLC) is achieved, along with lower consumption of organic solvents and comparable sensitivity. The method by Reddy *et al.*[8] requires 10.6 min per analysis without reported sensitivity parameters, whereas a LOD of 31.2 ng mL^{-1} is achieved with the current method in a shorter analysis time. The HPLC method by Johnson *et al.*[10] offers similar sensitivity (LOD 25.41 ng mL^{-1}) and analysis time (2.258 min); however, it is limited to plasma matrices and requires organic mobile phases.

LC-MS/MS techniques[11,12] demonstrate higher sensitivity with LODs in the nanomolar range; however, they are associated with sophisticated and expensive instrumentation that is not widely available in routine analysis laboratories. These methods also involve complex sample preparation procedures and specialized technical expertise. In contrast, the current method can be performed using commonly available reagents and conventional spectrofluorimetric instrumentation while maintaining suitable sensitivity for pharmaceutical and biological analysis.

The electrochemical method by Ghalkhani *et al.*[13] yields high sensitivity (LOD 2 nM) but relies on complex electrode modification procedures using nanomaterials that may be difficult to reproduce consistently. Similarly, fluorescence methods based on nanomaterials, such as gold nanoparticles[15] and Zn-MOF,[16] demonstrate high sensitivity but require specialized synthesis and characterization of nanomaterials. The method by Ibrahim *et al.*[14] using SDS or Al^{3+} shows similar LODs to the current approach; however, it is restricted to pharmaceutical tablets and requires either surfactant optimization or metal complexation. The SDS method may also suffer from micelle instability, while the Al^{3+} complexation approach requires precise pH control and involves aluminum compounds that require proper handling and disposal protocols.

A significant advantage of the current method is its applicability across different sample matrices, including pharmaceutical formulations, plasma, and environmental water samples, with good recovery rates and minimal matrix effects. The straightforward sample preparation, using only protein precipitation for plasma and salting-out extraction for water samples, makes it suitable for routine analysis. Additionally, specialized nanomaterials or complex instrumentation are not required, making the method accessible to standard analytical laboratories. The reasonable sensitivity, rapid analysis time, and environmentally friendly approach position this method as a practical alternative for the routine analysis of raloxifene in various matrices.

3.8. Greenness and blueness assessment

The greenness and practical applicability of the proposed erythrosine B-based fluorescence quenching method were assessed using established analytical assessment tools: the Analytical GREEnness (AGREE) calculator[27] and the Blue Applicability Grade Index (BAGI).[28]

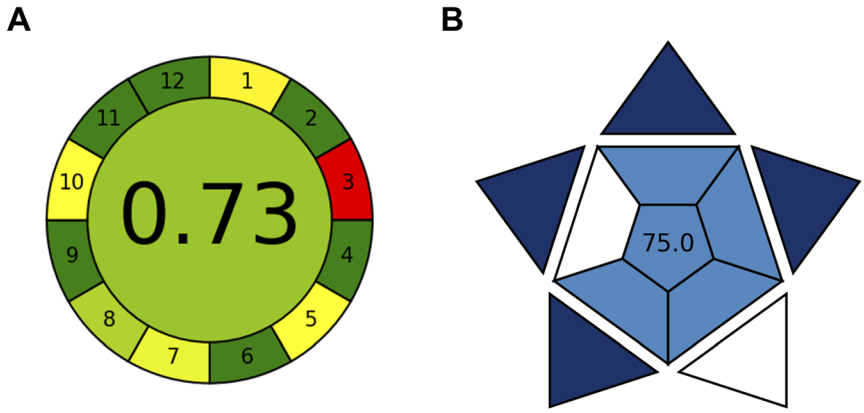

Fig. 6 (A) AGREE (Analytical GREEnness) calculator results with an overall score of 0.73, illustrating compliance with green analytical chemistry principles; (B) BAGI (Blue Applicability Grade Index) evaluation with a score of 75.0, confirming practical applicability for routine analysis.

The AGREE evaluation (Fig. 6A) revealed an overall greenness score of 0.73, indicating compliance with green analytical chemistry principles. The method performed well in several aspects of greenness. The absence of derivatization agents (principle 6) was observed, which eliminates additional reagent consumption and waste generation associated with derivatization procedures. Low energy consumption (principle 9) was achieved compared to instrumentation-intensive techniques, such as LC-MS/MS, and minimal hazardous chemicals were utilized, benefiting operator safety (principle 12). The method was also characterized by a minimized sample size and the absence of highly toxic reagents (principles 2, and 11). Areas for potential improvement were identified in principles 3, 5, and 10, specifically in developing *in situ* measurement capabilities, increasing automation and miniaturization of the method, and incorporating reagents from renewable sources.

The BAGI evaluation (Fig. 6B) yielded a score of 75.0, exceeding the recommended threshold of 60 for practical method implementation. The method was found to provide quantitative information, utilize widely available laboratory instrumentation, require straightforward sample preparation, and employ common commercially available reagents. Adequate pre-concentration efficiency was achieved, meeting the required sensitivity with a single extraction step, and reasonable sample volumes were utilized. Potential enhancements were identified in automation degree and multi-analyte detection capabilities that could be developed for high-throughput scenarios. Overall, the method demonstrated a favorable balance between environmental sustainability and practical applicability, making it suitable for implementation in laboratories with varying resource constraints while maintaining acceptable environmental impact compared to conventional techniques for raloxifene determination.

4. Conclusions, limitations and future perspectives

This study successfully developed a turn-off fluorescence sensor based on erythrosine B for the detection of raloxifene with significant analytical merits. The method exploits the static quenching mechanism ($K_{SV} = 4.87 \times 10^5$ M^{-1}) through a 1 : 1 complex formation, confirmed by Job's method and characterized by favorable thermodynamic parameters ($\Delta G = -32.45$ kJ mol^{-1}). Quantum mechanical calculations revealed strong binding interactions with a binding energy of −0.143391 hartree and a significant reduction in dipole moment (from 14.06 and 21.85 debye to 9.83 debye). Under optimized conditions (pH 4.0, 1.5 mL acetate buffer, 20.0 μg per mL erythrosine B), the method demonstrated excellent linearity (0.1–3.0 μg mL^{-1}, $r^2 = 0.9997$), sensitivity (LOD = 0.0312 μg mL^{-1}), and recoveries across different matrices (99.80% for pharmaceutical formulations, 95.55–103.03% for plasma, and 94.62–103.30% for environmental samples). The approach offers significant advantages over existing methods, including rapid analysis time (3 min *versus* 5–10 min for HPLC methods), comparable sensitivity, and minimal organic solvent consumption, as confirmed by favorable greenness (AGREE = 0.73) and applicability (BAGI = 75.0) scores.

Despite these advantages, this study has certain limitations that should be acknowledged. The fluorescence quenching approach using erythrosine B, while sensitive and practical, shares a common limitation with most fluorescence-based probes, including eosin Y, rhodamine B, and carbon quantum dots: the potential for non-specific interactions with multiple analytes through similar physicochemical processes. This selectivity challenge extends beyond fluorescence methods to other analytical techniques, where even well-established methods like HPLC-UV may lack sufficient selectivity for drugs with similar chromophores and retention behaviors, and electrochemical methods face similar challenges with compounds having similar redox potentials. While LC-MS/MS offers superior selectivity through mass-to-charge ratio identification, it comes with significantly higher costs and complexity. Additionally, while the current sample preparation techniques achieve adequate recoveries (>94%), potential interference from other strong quenchers with similar binding affinity to erythrosine B could affect accuracy in highly complex samples.

Future research should focus on developing more selective sample preparation techniques, particularly molecularly imprinted polymers (MIPs) specifically designed for the detection of raloxifene. MIPs could be engineered with specific recognition sites complementary to the molecular structure of raloxifene, enabling selective extraction and pre-concentration while effectively removing potential interferents. This approach would combine the molecular recognition capabilities of MIPs with the sensitivity and simplicity of the fluorescence method, potentially achieving selectivity comparable to more expensive techniques while maintaining cost-effectiveness. Additional directions include investigating alternative fluorophores with different binding mechanisms, extending applicability to metabolite determination (particularly glucuronide conjugates), and exploring miniaturization for high-throughput or point-of-care applications. These advancements would further enhance the utility of fluorescence-based approaches for raloxifene detection in pharmaceutical, clinical, and environmental analyses.

Data availability

The authors confirm that the data supporting the findings of this study are available within the article and its ESI file.†

Conflicts of interest

There are no conflicts of interest to declare.

Acknowledgements

The authors extend their appreciation to Taif University, Saudi Arabia, for supporting this work through project number (TU-DSPP-2024-57).

References

1 S. Martinkovich, D. Shah, S. L. Planey and J. A. Arnott, *Clin. Interventions Aging*, 2014, 1437–1452.
2 J. R. C. Rey, E. V. Cervino, M. L. Rentero, E. C. Crespo, A. O. Álvaro and M. Casillas, *Open Orthop. J.*, 2009, **3**, 14.
3 B. Ettinger, D. M. Black, B. H. Mitlak, R. K. Knickerbocker, T. Nickelsen, H. K. Genant, C. Christiansen, P. D. Delmas, J. R. Zanchetta, J. Stakkestad, C. C. Glüer, K. Krueger, F. J. Cohen, S. Eckert, K. E. Ensrud, L. V. Avioli, P. Lips and S. R. Cummings, *JAMA, J. Am. Med. Assoc.*, 1999, **282**, 637–645.
4 S. R. Cummings, S. Eckert, K. A. Krueger, D. Grady, T. J. Powles, J. A. Cauley, L. Norton, T. Nickelsen, N. H. Bjarnason, M. Morrow, M. E. Lippman, D. Black, J. E. Glusman, A. Costa and V. C. Jordan, *JAMA, J. Am. Med. Assoc.*, 1999, **281**, 2189–2197.
5 B. W. Walsh, L. H. Kuller, R. A. Wild, S. Paul, M. Farmer, J. B. Lawrence, A. S. Shah and P. W. Anderson, *JAMA, J. Am. Med. Assoc.*, 1998, **279**, 1445–1451.
6 G. C. Davies, W. J. Huster, Y. Lu, L. J. Plouffe and M. Lakshmanan, *Obstet. Gynecol.*, 1999, **93**, 558–565.
7 D. Hochner-Celnikier, *Eur. J. Obstet. Gynecol. Reprod. Biol.*, 1999, **85**, 23–29.
8 P. V. Reddy, B. S. Rani, G. S. Babu and J. V. L. N. S. Rao, *J. Chem.*, 2006, **3**, 713569.
9 Z. Y. Yang, Z. F. Zhang, X. B. He, G. Y. Zhao and Y. Q. Zhang, *Chromatographia*, 2007, **65**, 197–201.
10 A. P. Johnson, S. L. Jyothi, P. R. H. Vikram, K. Pramod, M. P. Venkatesh, R. A. M. Osmani and H. V. Gangadharappa, *Microchem. J.*, 2024, **201**, 110541.
11 T. Trdan, R. Roškar, J. Trontelj, M. Ravnikar and A. Mrhar, *J. Chromatogr. B*, 2011, **879**, 2323–2331.
12 T.-T. Chen, T.-Y. Huang, R.-N. Pan, G.-P. Chang-Chien and M.-C. Hsu, *J. Anal. Toxicol.*, 2013, **37**, 345–350.
13 M. Ghalkhani, S. Shahrokhian and M. Navabi, *Mater. Chem. Phys.*, 2021, **263**, 124131.
14 F. Ibrahim, N. El-Enany, R. El-Shaheny and I. Mikhail, *J. Mol. Liq.*, 2018, **252**, 408–415.
15 Y. Wu, X. Jin, E. Ashrafzadeh Afshar, M. A. Taher, C. Xia, S.-W. Joo, T. Mashifana and Y. Vasseghian, *Chemosphere*, 2022, **305**, 135392.
16 R. R. Madvar and M. A. Taher, *Environ. Res.*, 2024, **240**, 117449.
17 M. Garland, J. J. Yim and M. Bogyo, *Cell Chem. Biol.*, 2016, **23**, 122–136.
18 S. M. Derayea and D. M. Nagy, *Rev. Anal. Chem.*, 2018, **37**, 20170020.
19 M. Tolba and M. Salim, *Spectrochim. Acta, Part A*, 2021, **263**, 120156.
20 S. M. Derayea, A. A. Hamad, R. Ali and H. R. H. Ali, *Microchem. J.*, 2019, **149**, 104024.
21 S. M. Derayea, M. Oraby, A. A. S. Zaafan, A. A. Hamad and D. M. Nagy, *RSC Adv.*, 2024, **14**, 8283–8292.
22 M. Szabelski, D. Ilijev, P. Sarkar, R. Luchowski, Z. Gryczynski, P. Kapusta, R. Erdmann and I. Gryczynski, *Appl. Spectrosc.*, 2009, **63**, 363–368.
23 F. Ibrahim, R. Aboshabana and H. Elmansi, *R. Soc. Open Sci.*, 2022, **9**, 220628.
24 M. A. Abdel-Lateef, R. J. Darling and I. A. Darwish, *Luminescence*, 2024, **39**, e4777.
25 *ICH Guideline*, ICH, Geneva, Switzerland, 2022.
26 N. Boens, W. Qin, N. Basarić, J. Hofkens, M. Ameloot, J. Pouget, J.-P. Lefevre, B. Valeur, E. Gratton and M. Vandeven, *Anal. Chem.*, 2007, **79**, 2137–2149.
27 F. Pena-Pereira, W. Wojnowski and M. Tobiszewski, *Anal. Chem.*, 2020, **92**, 10076–10082.
28 N. Manousi, W. Wojnowski, J. Płotka-Wasylka and V. Samanidou, *Green Chem.*, 2023, **25**, 7598–7604.